CHAPTER 67

Application of The Second-order Mode Coupling Equation
to Coastal Engineering Problems

Mitsuhiro Tanaka†

Abstract

The Second-order Mode Coupling Equation (SMCE) is applied
to the 3-dimensional evolution of a solitary wave the crest-line
of which is not straight but bent initially. It is found that the
bent solitary wave recovers a straight crest-line spontaneously
by producing a nonuniform distribution of waveheight and hence
that of propagation speed along the crest-line.

1. The Second-Order Mode Coupling Equation

1.1 The Mode Coupling Equation

As pointed out by Zakharov(1968), the motion of water waves
can be expressed as a Hamiltonian system by using the total en-
ergy as the Hamiltonian and the complex amplitude spectrum
$b(\vec{k}, t)$ defined by

$$b(\vec{k}, t) = \sqrt{g/2\omega(k)}\, \tilde{\eta}(\vec{k}, t) + i\sqrt{\omega(k)/2g}\, \tilde{\phi}^s(\vec{k}, t) \qquad (1)$$

as the canonical variable. Here $\tilde{\eta}(\vec{k}, t)$ and $\tilde{\phi}^s(\vec{k}, t)$ are the Fourier
transform of the free surface displacement $\eta(\vec{x}, t)$ and the velocity
potential $\phi(\vec{x}, z, t)$ evaluated at the free surface respectively, and
$\omega(k) = \sqrt{gk\tanh kh}$, with $k = |\vec{k}|$.

† Assistant, Department of Applied Mathematics, Faculty of
Engineering, Gifu University 1–1 Yanagido, Gifu 501–11 JAPAN

When the Hamiltonian is approximated by a power series of $b(\vec{k}, t)$ truncated at the (n+1)th-order, the resulting Hamilton's equation which governs the evolution of $b(\vec{k}, t)$ contains n-th power of $b(\vec{k}, t)$ and is called here the n-th-order mode coupling equation.

In the derivation of the mode coupling equation, it is usually assumed that the nonlinearity of the underlying wave field is small (i.e., $ak \ll 1$) and that the bottom is flat (i.e., $h = $ const.) and impermiable. With regard to the value of kh, however, no assumption is made and the equation can be applied to waves of any wavelength so long as the above-mentioned assumptions hold.

The third-order mode coupling equation reduces to the well-known Zakharov's equation if only the near resonant interactions are taken into account among all the possible four-wave interactions. Zakharov's equation is further simplified to give the nonlinear Schrödinger equation when the assumption of narrow-bandedness of the wave field is added.

Here in this work, we forcus our attention to the Second-order Mode Coupling Equation which we'll call the SMCE for short. Following the notation of Stiassnie and Shemer(1984), the SMCE can be expressed as follows,

$$
\begin{aligned}
\frac{db(\vec{k})}{dt} &+ i\omega(k)b(\vec{k}) \\
&+ i \iint V^{(1)} b(\vec{k}_1) b(\vec{k}_2) \delta(\vec{k} - \vec{k}_1 - \vec{k}_2) d\vec{k}_1 d\vec{k}_2 \\
&+ i \iint V^{(2)} b^*(\vec{k}_1) b(\vec{k}_2) \delta(\vec{k} + \vec{k}_1 - \vec{k}_2) d\vec{k}_1 d\vec{k}_2 \\
&+ i \iint V^{(3)} b^*(\vec{k}_1) b^*(\vec{k}_2) \delta(\vec{k} + \vec{k}_1 + \vec{k}_2) d\vec{k}_1 d\vec{k}_2 = 0. \quad (2)
\end{aligned}
$$

This equation reduces to the well-known K-dV equation under the assumptions that the water is shallow (i.e., $kh \ll 1$) and all the wave components propagate only in the positive x-direction.

There are two major reasons why we choose the SMCE here and discard all the higher order nonlinear interaction terms. The

first reason is; It can be shown that the magnitude of the third-order terms of the mode coupling equation relative to the second-order ones is given by the wave steepness ak of the underlying wave. This implies that the third-order terms as well as all the higher order terms would give only negligibly small contributions to the motion of a solitary wave which we focus our attention to in this work, because it is generally true for a long wave like a solitary wave that a/h may be $O(1)$ while kh is very small, resulting in a very small value of ak.

The second reason to choose SMCE is much more pragmatic. The n-th order mode-coupling equation generally contains n-tuple convolution sums, and the number of operations required per each time step would increase as N^n with N being the number of Fourier modes involved in the calculation. However, the operation count necessary for the evaluation of the second-order convolution terms increase only as $N \ln N$ instead of N^2. This is because these terms can be rewritten to a form to which the pseu-dospectral method is applicable and so can be evaluated fast by a series of FFT's and inverse FFT's. This reduction of the number of numerical operations becomes crucial when one is to persue a 3-dimensional problem like the one shown in Sec. 2 of this work, because for such a 3-D problem the number of Fourier modes required for a reasonably accurate expression of the wave field inevitably becomes large. For such a problem with large number of Fourier modes, the higher order mode coupling equations like Zakharov's equation, however valuable they may be from the the-oretical point of view, would require unrealistically vast amount of CPU time on the computing facilities now available and would have only a very limited practical value.

1.2 Accuracy of The SMCE

Before proceeding to an application of the SMCE to a practically interesting problem, it may be sensible to know how better the SMCE approximates the behaviour of long waves than the K-dV equation which is one of the most standard equations for long wave problems.

What we've done is to input the steady periodic solution of

fully nonlinear water wave equations to the SMCE and the K-dV as the initial condition and observe how strongly this steady profile is deformed at later times. In the calculation shown below, we tentatively fix the water depth so that $kh = 0.5$. For this value of kh, the linear dispersion relation of the K-dV equation $\omega(k) = \sqrt{ghk}\left\{1 - (kh)^2/6\right\}$ is a very good approximation of the exact one $\omega(k) = \sqrt{gk\tanh kh}$ with the error being only less than 0.3%. In this sense the water is sufficiently shallow and we expect that the K-dV equation approximates the steady translation very well.

The deformation of the wave form is measured by a quantity $D(t)$ defined by

$$D(t) = \int_0^L \{\eta(x,t) - H(x - ct)\}^2 \, dx \Big/ \int_0^L H^2 dx, \qquad (3)$$

where H is the profile of the steady periodic wave solution employed as the initial condition and c its propagation speed. As the initial condition is an exact steady solution of the fully nonlinear problem, the deformation $D(t)$ should remain zero if the approximation is 'ideal'. Therefore, we can discuss the accuracy of various different approximations by comparing the magnitude of $D(t)$ given by those approximations.
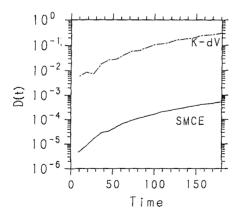

Fig. 1 Growth of Deformation $D(t)$ for a steady periodic solution with $ak = 0.1$ and $kh = 0.5$

Figure 1 shows the growth of $D(t)$ for the steady wave with $ak = 0.1$. It can be seen that $D(t)$ given by the SMCE remains about 500 times smaller than that of the K-dV equation during the period of time considered, implying that the SMCE gives 500 times more accurate result than the K-dV equation does, at least for the steady translation of the particular wave considered here. It may be noted that the length of time shown in Fig.1 is fairly long for the particular steady wave, and during which the wave has propagated more than 250 times the water depth.

If the nonlinear terms of both the SMCE and the K-dV are calculated by the pseudospectral method, and the time-stepping of both equations are carried out by Runge-Kutta-Gill method, the SMCE requires about three times longer CPU time than the K-dV equation does.

2. Three-Dimensional Evolution of A Bent Solitary Wave

2.1 Initial Condition

As an application of the SMCE to a 3-dimensional problem, we investigate the time evolution of a wave which is basically a Boussinesq solitary wave propagating in the positive x-direction but the crest-line of which is slightly bent initially. More specifically, we've prescribed the initial condition as follows:

$$\eta(x, y, 0) = a_0 \operatorname{sech}^2 \left\{ (x - x_c(y))/D \right\} \tag{4a}$$

$$\phi^s(x, y, 0) = \sqrt{4a_0/3} \tanh \left\{ (x - x_c(y))/D \right\} \tag{4b}$$

where D is the width of the solitary wave which is related to the waveheight a_0 by $D = \sqrt{4(1 + a_0)/3a_0}$. In the calculation reported here, the initial shape of the crest-line $x_c(y)$ is chosen tentatively as $x_c(y) = x_0 - \epsilon \cos(2\pi y/L_y)$ with x_0 being some appropriate constant. The parameter ϵ determines the magnitude of the y-variation of the crest position, while L_y determines its length-scale. For the sake of numerical computation, the wave field is assumed to be periodic both in the x- and y-direction with the period L_x and L_y, respectively. The period in the x-direction L_x is taken sufficiently long so that the existence of the

periodic boundary would not affect the evolution of the wave field seriously. The water depth is normalized as 1.

Figure 2 shows the bird's-eye view of the wave form at $t = 0$ (Fig. 2a) and $t = 30$ (Fig. 2b) when the crest is not bent initially. The values of parameters chosen for this calculation are $a_0 = 0.2$, $L_x = 61.3$, $L_y = 5$, $N_x = 128$, $N_y = 12$ and $\Delta t = 0.5$. Here N_x and N_y are the number of mesh points in the x- and y-direction, respectively, and Δt is the step-size of the time-integration which is carried out by Runge-Kutta-Gill scheme. The total CPU time is about 57 sec. on FACOM M780 of the Computation Center of Nagoya University. Although the initial condition is not a steady solution of the SMCE but of the Boussinesq equation, the solitary wave seems to be propagating almost steadily on the SMCE as well. This is quite reasonable because the Boussinesq soliton should be a good approximation of the steady solution of the SMCE when the waveheight is not large as in the present case where $a_0 = 0.2$.
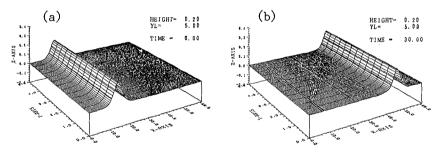

Fig. 2 Wave-form when the solitary wave is not bent initially.
(a) $t = 0$, (b) $t = 30$.

2.2 Scenario of 3-D Evolution

An example of the evolution of a bent solitary wave is shown in Fig. 3. All the parameters are the same as the previous case, the only difference being that the amplitude of the initial bend ϵ is set equal to 1 instead of 0. Figure 3a shows the bird's-eye view of the initial wave form, and the time evolution that follows is shown in Figs. 3b–3f. The scenario of the evolution may be summarized as follows:
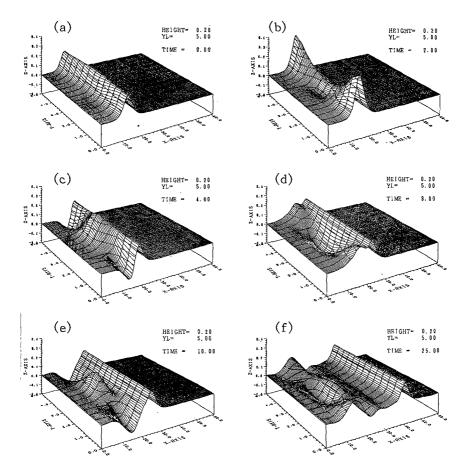
Fig. 3 3-D evolution of a bent solitary wave. $a_0 = 0.2$, $L_y = 5$ and
$\epsilon = 1$.

(1) The waveheight spontaneously starts to increase around $y = 0$
and $y = L_y$ where the wave crest is made behind initially, while
it starts to decrease around $y = L_y/2$ where the crest is put
forward. As it is generally true for long waves that the higher
waves propagate faster than the lower, this unevenness of the
waveheight brings out such a distribution of propagation speed
along the crest-line that would help the bent crest-line go back to
a straight line. (Fig.3b)

(2) Around $y = 0$ and $y = L_y$ where the crest is now propagating faster because of the increased waveheight, the water just behind the crest appears not to be able to keep up with the crest, and as a result of that, a depression of water surface appears. On the other hand, around $y = L_y/2$, the water just behind the crest seems to be overtaking the crest which is now propagating by a reduced speed, and a swell up of water surface is observed behind the crest. (Fig.3c)

(3) The lateral distribution of the free surface displacement behind the crest-line that has appeared in (2) evolves into a standing wave-like oscillation. The period of oscillation coincides approximately with that of a linear long wave with wavenumber $k = 2\pi/L_y$. By this time, the recovery of a straight crest-line has been accomplished, and a 2-dimensional solitary wave with a straight crest-line is emerging out of the traisient wave motion. (Figs.3d and 3e)

(4) The initial condition finally splits into two parts. One is a 2-D solitary wave with a straight crest-line which propagates steadily with a speed given approximately by $1 + a/2$, and the other is a standing wave-like oscillation which appears to stay around the position for all the time, the position where the wave was given initially. This difference between the propagation speed of these two parts brings out the appearance of a region with a calm free surface between them. This calm region grows wider as time goes on and the solitary wave propagates further from the initial position. (Fig.3f)

Figure 4a shows the top-view of the crest-line at various time-steps in which it can be seen clearly how the crest-line approaches a straight line. In order to see this phenomenon more quantitatively, we show in Fig.4b the evolution of a quantity X_{dev} defined by

$$X_{\mathrm{dev}}(t) = \int_0^{L_y} \{x_c(y) - \overline{x_c}\}^2 \, dy, \qquad (5)$$

where $x_c(y)$ is the x–coordinate of the crest-line in terms of y and $\overline{x_c}$ is the average of $x_c(y)$. By its definition, X_{dev} vanishes when the crest-line is straight.
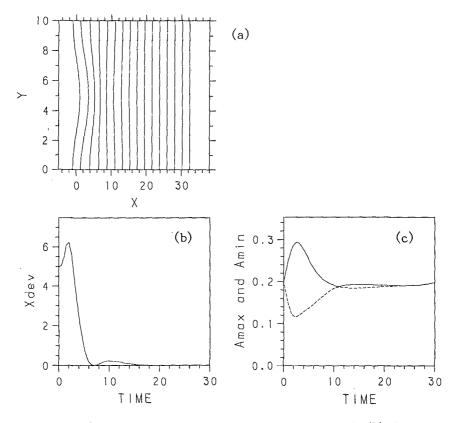
Fig. 4 (a) The top-view of the crest-line for $0 \leq t \leq 30$. (b) X_{dev}, i.e., the deviation of the crest-line from a straight line. (c) The evolution of the maximum and the minimum waveheight along the crest-line ($a_0 = 0.2$, $L_y = 10$ and $\epsilon = 1$)

Figure 4c shows the evolution of the maximum and the minimum waveheight along the crest-line. This figure shows clearly the spontaneous appearance of a nonuniformity of the waveheight right after the initial time, as well as its gradual relaxation and the return to a state of uniform waveheight.

2.3 L_y – Dependence

We've shown above that a solitary wave seems to have an ability to make its crest-line straight when it's bent initially by producing a nonuniform distribution of the waveheight along the crest.

There are two important quantities that characterize this phenomenon. One is the characteristic time-scale of the phenomenon and the other is the size of the highest wave that appears during the transient motion. Figure 5a shows the L_y-dependence of the characteristic time-scale which is defined as the time when $X_{dev}(t)$ of eq.(5) attains its first local minimum. In the same figure is also shown by a dashed line the period of oscillation of a linear long wave with wavelength L_y. The result shows that the longer the length-scale of the initial bend, the longer it takes to return to a straight crest-line.
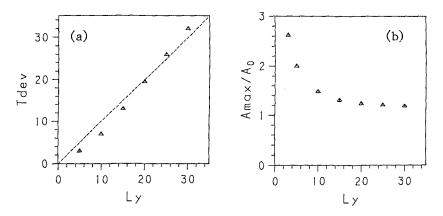

Fig. 5 (a) L_y-dependence of the characteristic time-scale (b) L_y-
      dependence of the maximum waveheight that appears during
      the transient motion

The maximum waveheight that appears during the transition divided by the initial height is shown in Fig.5b as a function of L_y. This figure shows that the higher wave appears as the length-scale of the initial bend is shortened or as the curvature of the initial crest-line is increased. For the type of initial condition we are now using, we can get a wave which is 2.6 times as high as the initial wave by bending its crest-line such that $L_y=3$ and $\epsilon = 1$. This result strongly suggests that it might be possible to make a solitary wave break without decreasing the water depth but by just bending its crest-line somehow. We've also investigated the dependence of the phenomenon on the initial waveheight a_0

by changing a_0 from 0.1 to 0.5, but no appeaciable change in the characteristic time-scale or the maximum waveheight was observed.

The crest-line of solitary waves that are observed on the beach are usually very long and nearly straight in spite of the uneven bottom topography over which they may have propagated. This might be related to the ability of a solitary wave as that shown above to keep its crest-line straight by adjusting the waveheight distribution along the crest when it is deformed by some external cause.

3. A Simple Model

In this section, we try to reproduce the phenomenon shown in the previous section by a simple model in order to understand intuitively the principle that underlies the phenomenon. The model the detail of which is explained below is derived by an analogy with the motion of an axisymmetric (or cylindrical) solitary wave.

The waveheight of a diverging axisymmetric wave which can be produced quite easily by throwing a stone into a pond is observed to decrease as the wave propagates outward and the crest-line of the wave is stretched. On the other hand, the waveheight of a converging axisymmetric wave which occurs when one hits a circular basin filled with water increases as the wave propagates inward and the crest-line is shortened. It is quite obvious that these changes of waveheight are the result of conservation laws.

3.1 Assumptions of the Model

Bearing this in mind, we now propose a very crude model to understand intuitively the 3-D evolution of a bent solitary wave. The followings are the assumptions on which the model is constructed;

(1) Each point that constitutes the crest-line moves in the direction normal to the crest-line at that point with velocity v given by $v = (1 + a/2)$, where a is the local waveheight of the crest.

(2) The waveheight a changes in such a way that *mass* or *energy* is conserved. (see Assumption (3) below.)

(3) The shape of normal cross-section at any point of the crest-line is similar to that of the K-dV soliton, and its horizontal length-scale is proportional to $1/\sqrt{a}$ when the local waveheight is a.

3.2 Evolution Equations

The shape of the crest-line and the distribution of the waveheight along it at time t is assumed to be described as $x = x(\sigma), y = y(\sigma)$ and $a = a(\sigma)$, where σ is a parameter which plays a role of the *Lagrangian* coordinate. With this parametric representation of the crest-line, the Assumption (1) can be expressed as

$$\left.\frac{\partial \vec{x}}{\partial t}\right|_{\sigma} = \vec{v} = \{1 + a(\sigma)/2\}\,\vec{n}, \tag{6}$$

with

$$\vec{n} = (y_\sigma \vec{i} - x_\sigma \vec{j})/\sqrt{x_\sigma^2 + y_\sigma^2}.$$

This is the evolution equation for the shape of the crest-line. On the other hand, the evolution of $a(\sigma)$ is governed by the Assumptions (2) and (3) which require the following relations to hold. When *mass* conservation is assumed,

$$a(x_\sigma^2 + y_\sigma^2) = \text{const.} \tag{7}$$

along a ray (i.e., $\sigma = $ const.), while

$$a^3(x_\sigma^2 + y_\sigma^2) = \text{const.} \tag{8}$$

if *energy* conservation is assumed instead.

3.3 Result

Figures 6.a and 6.b show the top-view of the crest-line at various times and the evolution of X_{dev} defined by eq.(5), respectively, that are obtained by the model with *energy* conservation. Al-thought the model is quite a crude one and there would be a lot of possibilities to elaborate on it, it nevertheless expresses, at least qualitatively, the approach of a bent crest-line to a straight line as shown by these figures.
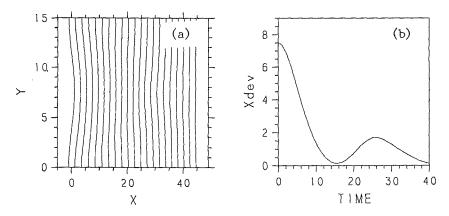
Fig. 6 (a) The top-view of the crest-line for $0 \leq t \leq 40$. (b) X_{dev},
i.e., the deviation of the crest-line from a straight line. (
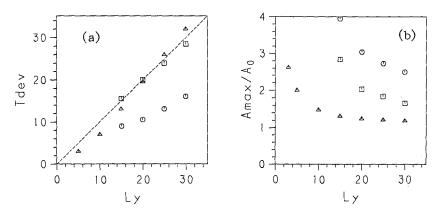$a_0 = 0.2$, $L_y = 15$, $\epsilon = 1$ and the *energy* conservation eq.(8)
is assumed.)

Fig. 7 (a) L_y-dependence of the characteristic time-scale (b) L_y-
dependence of the maximum waveheight that appears during
the transient motion. $\oplus$: model with *mass* conservation,
$\square$: model with *energy* conservation, $\triangle$: SMCE.

The L_y-dependence of the characteristic time-scale and the
maximum waveheight obtained by the present model are shown
in Figs. 7a and 7b respectively. In these figures, the open squares
show the result of the model with *energy* conservation, while the
open circles show that of the model with *mass* conservation. The

result of the SMCE is also shown in the same figures by open triangles for the sake of comparison.

It can be seen from these figures that the model with *energy* conservation generally gives much better results than the model with *mass* conservation. Especially, the characteristic time-scale predicted by the model with *energy* conservation almost coincides with that predicted by the SMCE as shown in Fig. 7a. This reminds us of the well-known fact in the perturbation theory of the K-dV equation that the amplitude modulation of one-soliton induced by a small perturbation can be calculated correctly by using any of the infinite number of conservation laws except the first one which corresponds to the mass conservation. This somewhat peculiar fact can be explained in terms of the non-secular condition of the perturbation analysis. (see for example Tanaka (1980))

References

STIASSNIE, M. AND SHEMER, L. (1984)
On modification of the Zakharov equation for surface gravity waves.
J. Fluid Mech. 143, 47–67.

TANAKA, M. (1980)
Perturbations on the K-dV solitons
– An approach based on the multiple time scale expansion –
J. Phys. Soc. Jpn. 49, 807–812.

ZAKHAROV, V.E. (1968)
Stability of periodic waves of finite amplitude on the surface of a deep fluid.
J. Appl. Mech. Phys. 2, 190–194.